Vol. 6, No. 2, April 2022, pp. 171-182

Current Optics and Photonics

Regular Paper

Design and Development of a Single-photon Laser and Infrared Common Aperture Optical System

Wu Hongbo[1,2,3], Zhang Xin[1,2], Tan Shuanglong[1,2,3]*, Liu Mingxin[1,2], Wang Lingjie[1,2], Yan Lei[1,2], Liu Yang[1,2], and Shi Guangwei[1,2]

[1]*Changchun Institute of Optics, Fine Mechanics and Physics, Chinese Academy of Sciences, Changchun 130033, China*
[2]*Key Laboratory of Optical System Advanced Manufacturing Technology, Chinese Academy of Sciences, Changchun 130033, China*
[3]*University of Chinese Academy of Sciences, Beijing 100039, China*

(Received November 29, 2021 : revised February 4, 2022 : accepted February 23, 2022)

A single-photon laser and mid-wave infrared (MWIR) common aperture optical system was designed and developed to detect and range a long-distance civil aviation aircraft. The secondary mirror of the Ritchey-Chretien (R-C) optical system was chosen as a dichroic lens to realize the design of a common aperture system for the laser and MWIR. Point spread function (PSF) ellipticity was introduced to evaluate the coupling efficiency of the laser receiving system. A small aperture stop and narrow filter were set in the secondary image plane and an afocal light path of the laser system, respectively, and the stray light suppression ability of the small aperture stop was verified by modeling and simulation. With high-precision manufacturing technology by single point diamond turning (SPDT) and a high-efficiency dichroic coating, the laser/MWIR common aperture optical system with a φ300 mm aluminum alloy mirror obtained images of buildings at a distance of 5 km with great quality. A civil aviation aircraft detection experiment was conducted. The results show that the common aperture system could detect and track long-distance civil aviation aircraft effectively, and the coverage was more than 450 km (signal-to-noise ratio = 6.3). It satisfied the application requirements for earlier warning and ranging of long-range targets in the area of aviation, aerospace and ground detection systems.

Keywords : Common aperture, Ellipticity, Middle wave infrared, Single-photon laser, Stray light
OCIS codes : (110.3080) Infrared imaging; (120.4570) Optical design of instruments; (140.0140) Lasers and laser optics; (220.0220) Optical design and fabrication; (220.4830) Systems design

I. INTRODUCTION

In recent years, the detection and surveillance of distant dimmer space targets have received much attention in the field of military defense. Target detection and identification have become increasingly difficult with the continuous advancement of optical detection technology, the increasing complexity and diversity of modern countermeasures, the increased level of various reconnaissance, camouflage and other techniques, and the increasing complexity of the application environment and scope. In addition, there is an urgent demand for weapon systems to obtain geometry, bearing, distance and movement pattern information of distant dimmer space targets.

Because the overall information of targets cannot be provided by a single detection mode, a new generation of multimode composite detection systems has been proposed. Composite multimode detection technology has become

*Corresponding author: 15567408408@126.com, ORCID 0000-0001-5627-8499

Color versions of one or more of the figures in this paper are available online.

a research hotspot among scholars worldwide. Zhang *et al*. [1–3] designed a dual-band imaging system of visible light and longwave infrared. Because infrared imaging is characterized by a long detection distance, high detection accuracy and sensitivity, along with comprehensive target information, such as the target's shape and basic structure, can be obtained in an intuitive manner. Composite infrared and laser detection systems have been extensively applied in detection systems for distant dimmer space targets. By integrating the target bearing information obtained from infrared images and the target distance information obtained from laser ranging, the target geometry, distance, bearing and motion morphology can be effectively acquired. To achieve a longer detection distance and a larger data sampling rate, exploration of single-photon laser ranging technology has been conducted worldwide. This ranging technology features high sensitivity, low power consumption and high detection efficiency, especially in remote ranges with a distance greater than 100 km [4].

However, its performance is significantly affected by background noise. Song and Wang *et al*. [5, 6] conducted an investigation of infrared and laser composite detection technology. Many scholars have developed composite detection with lasers and infrared using the design method of common apertures [7–12]. Generally, after common aperture receiving, the dichroic process of the laser and infrared should be performed in a parallel optical path or a quasi-parallel optical path. This is a complex structure that is not conducive to the suppression of clutter in the laser channel and background radiation in the infrared channel. Hence, it is not suitable for single-photon laser detection.

In this study, a composite detection system of medium-wave infrared imaging and single-photon laser ranging was adopted to obtain higher detection sensitivity and ranging performance for long-distance civil aviation aircraft. A dichroic method in a converging optical path and stray light elimination technology by a small aperture stop were adopted to design a laser/infrared common aperture detection system. With high-precision manufacturing technology by single point diamond turning (SPDT) and a high-efficiency dichroic coating, the laser/mid-wave infrared (MWIR) common aperture optical system was well manufactured and assembled. According to the experimental results, the laser/infrared composite detection system is capable of clear imaging and long-range detection. This method can be extensively applied in aviation, aerospace and ground early warning detection fields.

II. PRINCIPLES

2.1. Working Principle

The laser and infrared common aperture detection system is composed of a primary system, an infrared module and a laser module. The working principle of this system is presented in Fig. 1.

The medium-wave infrared radiation energy and laser echo signal of the target are received by the large aperture primary mirror of the primary system; the dichroic process is performed in the converging optical path on the first surface of the secondary mirror so that the medium-wave energy can be reflected to the infrared module, and the laser is simultaneously transmitted to the laser channel. The medium-wave infrared imaging optical path remains coaxial with the primary system, while the laser receiving optical path is folded twice by turning mirrors after the dichroic process. The final receiving end is located above the primary system. Therefore, the laser receiving the optical path will not generate an extra central obstruction.

2.2. Principle of Distant Ranging Technology with a Single-photon Laser

Single-photon laser ranging is realized with highly

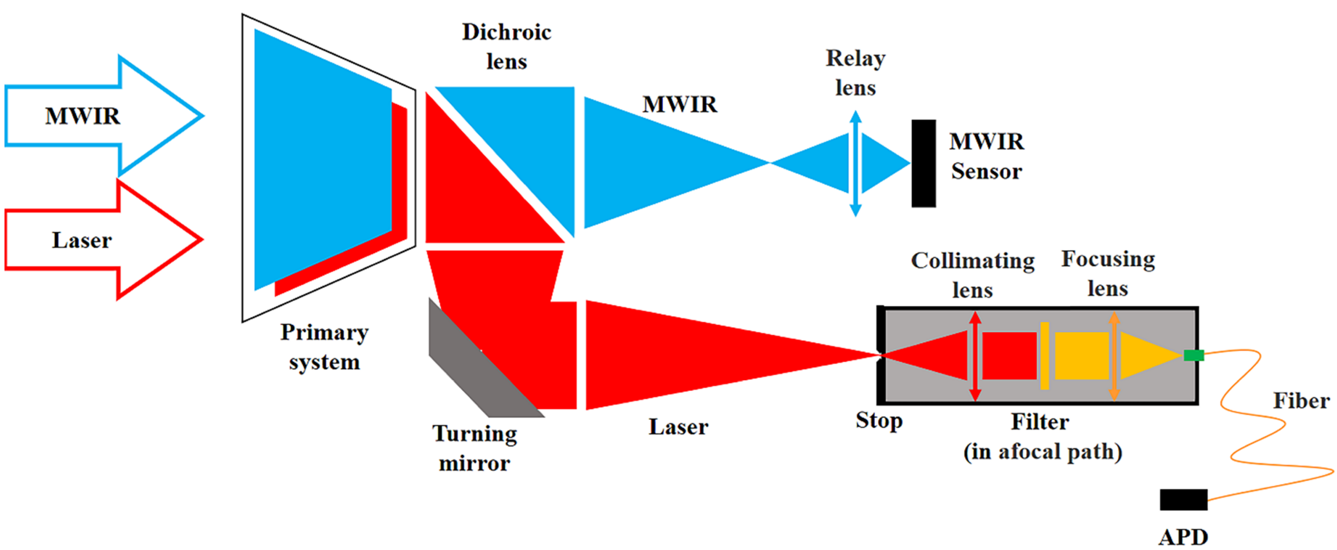

FIG. 1. Schematic diagram of working principle.

sensitive single-photon detection technology and time-related single-photon counting technology, which refers to mathematical statistics for the echo signal to get the target distance. The principle of photon counting is shown in Fig. 2, as a schematic diagram.

High speed echo signal sampling and background light noise suppression are realized with the help of high-speed signal acquisition technology and data processing technology. By using the idea of mathematical statistics, the extremely weak signal light is extracted from the background noise to ensure the detection probability of the system. Therefore, compared with traditional ranging technology, the measurement performance of photon counting laser ranging technology is more excellent.

The echo photons corresponding to each laser pulse are detected and stored first. Subsequently, the sampling results of the multiple pulses are accumulated; then, the specific corresponding relationship between the echo signal and the pulse signal's time window can be judged based on the accumulated results. Because the quantity of photons in different time windows after accumulation is different, the arrival time of the laser pulse echo can be accurately calculated. Then, the distance to be measured can be obtained [13, 14].

2.3. Analysis of Target Radiation Characteristics and Operating Range

The main radiation in the medium-wave band (3.7 μm–4.8 μm) of civil aviation aircraft mainly originates from three parts: nose, engine and plume. During flight, the target temperature level ranges from 260 K to 390 K. According to the Stefan-Boltzmann law, the radiation intensity is approximately 8 W/sr at a target temperature of 300 K [15, 16]. The system aperture can be calculated according to the formula with respect to point-target detection [17, 18].

$$R^2 = \frac{\Delta I \cdot \tau_{ao} \cdot A_{\mathrm{o}} \cdot \tau_o \cdot D_p{}^*}{N_t \cdot (A_{\mathrm{d}} \cdot \Delta f)^{1/2} \cdot \mathrm{SNR}} \exp\left(-\sigma R\right), \quad (1)$$

where R is the working distance in km; ΔI is the difference in radiation intensity in W/sr; A_o is the entrance pupil area in cm^2; SNR is the threshold of the signal-to-noise ratio; D_p* is the specific detection rate of the sensor, in cm • Hz$^{1/2}$ • W^{-1}; τ_{ao} and τ_o are the transmittance of atmospheric and optical systems, respectively; N_t is the quantity of dispersion pixels; Δf is the equivalent noise bandwidth of the sensor in Hz; A_d is the sensor area in cm^2; and σ is the atmospheric extinction coefficient in km^{-1}.

To realize high signal-to-noise ratio (SNR ≥5) passive detection of civil aviation aircraft at a long distance (not less than 400 km), the system aperture must not be less than 275 mm owing to the influence of factors such as central obstruction, system efficiency, atmospheric absorption and stray light.

III. DESIGN OF LASER/INFRARED COMMON APERTURE SYSTEM

3.1. Design Parameters

Parameters of the MWIR system:

1) Wave bands: 3.7–4.8 μm;
2) Effective aperture diameter: 280 mm;
3) F/#: 2;
4) Sensor parameters: 640 × 512, 25 μm;

Parameters of laser system:

1) The diameter of the receive aperture: 280 mm;
2) Wavelength: 1064 nm;
3) The core diameter of the receiving fiber: 200 μm;
4) The fiber numerical aperture: NA = 0.2;

3.2. Design of the Infrared Optical System

To realize the dichroic design of laser and medium-wave bands with a small volume, a Ritchey-Chretien (R-C) optical system was selected as the initial structure to optimize the design [19–23]. In addition, a secondary mirror was employed to perform the dichroic lens process for the laser and infrared channels, which solved dual-band high-efficiency dichroic problems and realized the miniaturization design

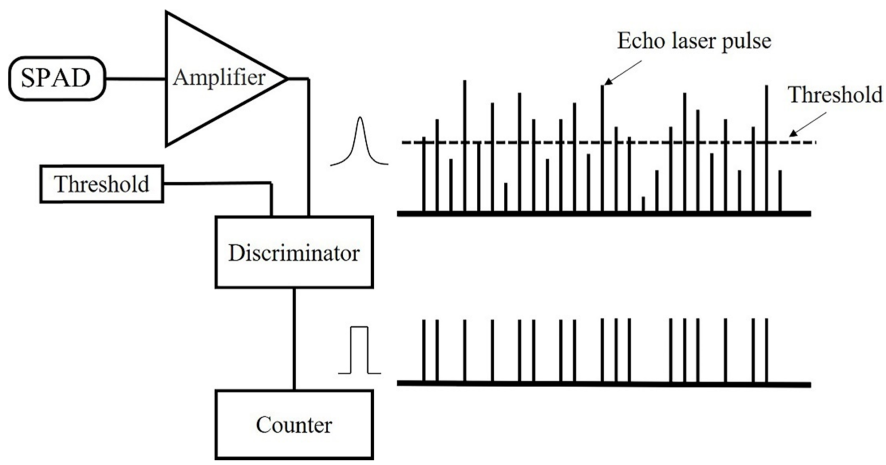

FIG. 2. Schematic diagram of photon counting.

of the system. In the design process, the first image plane of the infrared optical path was controlled in front of the vertex of the primary mirror, which reduced the influence of the central obscuration of the primary mirror on optical efficiency. Furthermore, a rectangular field stop was placed in the first image plane to improve the suppression of stray radiation of the system. The infrared imaging module consists of a primary mirror, a secondary mirror and an MWIR lens group with four lenses. The primary mirror is made of an aluminum alloy, the secondary mirror is made of silica, and the MWIR lens group lenses are made of silicon, silicon, germanium and silicon, respectively. The front surface of the germanium lens is designed as an aspheric surface to calibrate the off-axis aberration. An optical path diagram of the optimized infrared optical system is shown in the Fig. 3.

Figures 4 and 5 present the image quality design of the infrared optical system. Among them, the modulation transfer function (MTF) is close to the diffraction limit, and the encircled energy of a single pixel is better than 65%, which is necessary for detecting distant targets with a higher sensitivity.

3.3. Design of the Laser Optical System

A coaxial catadioptric structure was adopted in the laser receiving optical system, as in the structural schematic diagram shown in Fig. 6. To meet the high requirement of the single-photon detector for stray light suppression in the system, a secondary image plane was designed in front of the

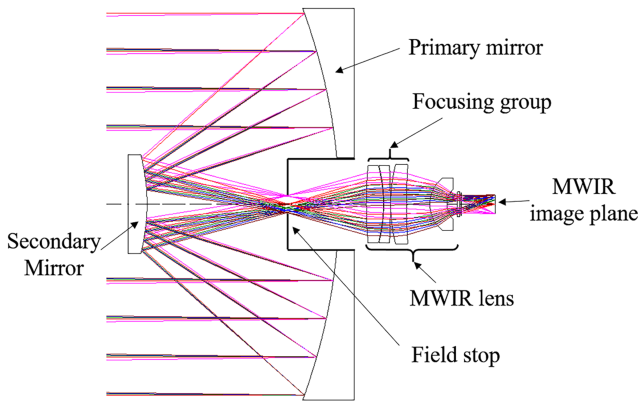

FIG. 3. Layout of the MWIR optical system.

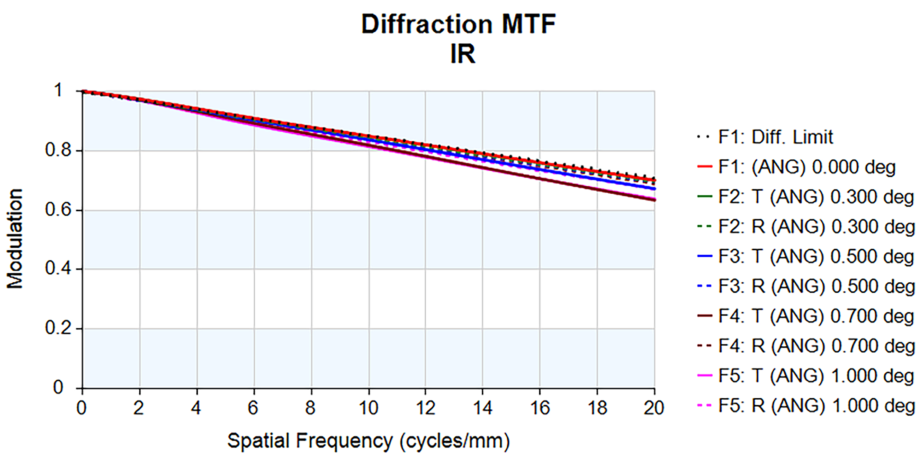

FIG. 4. Curve of the modulation transfer function (MTF).

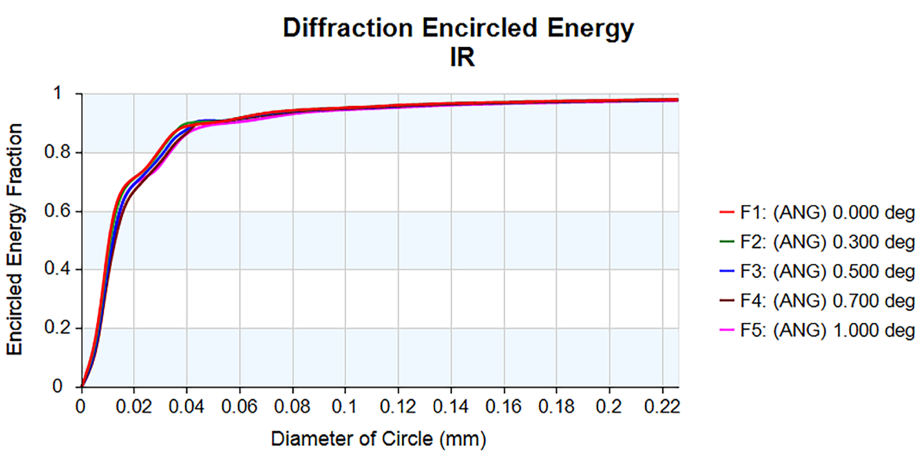

FIG. 5. Curve of the encircled energy.

back-end laser receiving lens group, and a small aperture stop was arranged on the secondary image plane. The aperture stop will not block the optical path of the primary system, and the suppression of stray light in the laser optical path can be realized efficiently without affecting the detection ability of the primary system. To improve the working efficiency of the narrow bandpass filter, an afocal light path was designed in the second part of the laser receiving lens, as shown in Fig. 4.

Encircled energy and geometrical spots of the laser receiving optical system are shown in Figs. 7 and 8. These two important indices reached the diffraction limit, which can be employed to receive single-photon laser energy with high efficiency.

Since a fiber with a diameter of φ200 μm was used as the laser receiver, the coupling efficiency was greatly affected by the shape of the energy distribution on the receiving fiber face. In this paper, point spread function (PSF) ellipticity was adopted to evaluate the PSF shape on the laser image plane. PSF ellipticity is a very important index in astronomical optical systems and is usually not greater than 0.15. The requirement of PSF ellipticity has also been applied to laser receiving systems. PSF ellipticity is defined as a function of weighted quadrupoles

$$Q_{ij}^{W} = \frac{\int I(x,y)\,x_i x_j W(x,y)\,dxdy}{\int I(x,y)\,W(x,y)\,dxdy}, \tag{2}$$

where W(x, y) is a Gaussian weight function of scale length r_g (r_g is some measure of the PSF size, such as the half-light radius) and $x_1 = x - \bar{x}$, $x_2 = y - \bar{y}$. An ellipticity e and its size

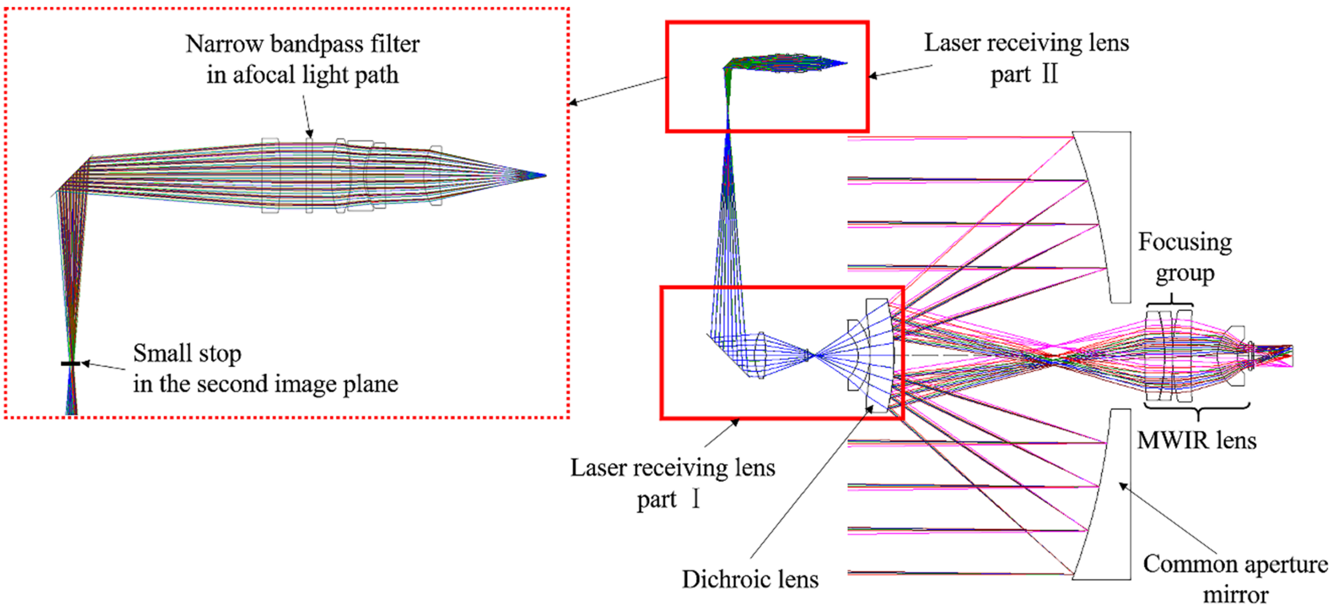

FIG. 6. Layout of the laser receiving system.

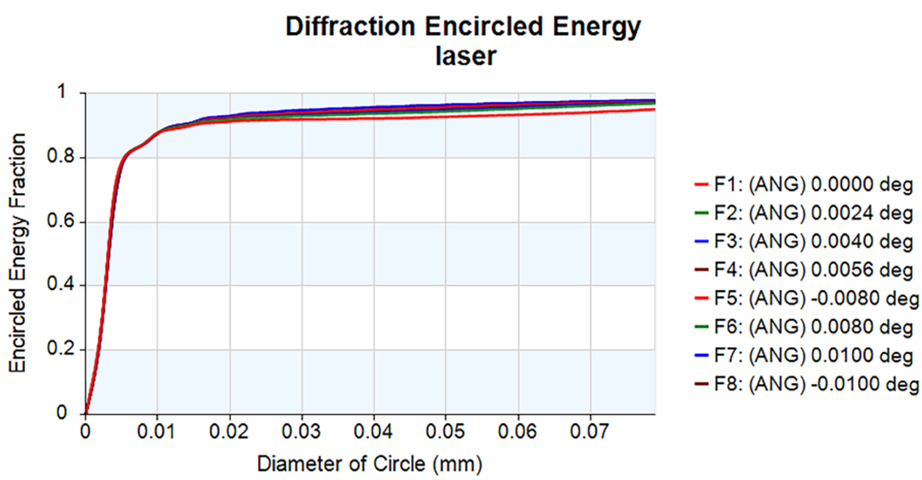

FIG. 7. Curve of the encircled energy.

R are defined from these weighted moments using

$$e = \frac{Q_{xx}^W - Q_{yy}^W + 2iQ_{xy}^W}{Q_{xx}^W + Q_{yy}^W} = e_1 + ie_2, \tag{3}$$

$$R = \sqrt{Q_{xx}^W + Q_{yy}^W}. \tag{4}$$

The PSF ellipticity and the PSF size of the laser receiving system in each field of view were calculated according to the above definition, as shown in the Table 1.

The coupling efficiency is the fraction of the radiation energy coupled to the receiving fiber from the source which is the product of the system efficiency (which is determined by the NA and optical efficiency) and receiving efficiency (which is determined by the NA and aberration of the receiving fiber). The coupling efficiency of the laser receiving system was also analyzed against the PSF ellipticity in each field of view. The optical efficiency was assumed to be 0.85 in all fields of view, and the results are shown in Table 1. The results showed that the coupling efficiency was more related to the PSF shape than to its size. Therefore, PSF ellipticity should be considered when designing laser receiving systems with a receiving fiber.

3.4. Stray Light Analysis of the Laser Receiving System

In this study, the suppression ability of the laser receiving system for stray light was simulated and analyzed, and point source transmittance (PST) was adopted as the evaluation index. The stray light simulation model of the system is shown in Fig. 9. The simulation results at different incident angles (θ) are listed in Table 2. PST-1 and PST-2 represent the PST of the laser receiving system without and with the aperture stop, respectively. The PST of the laser receiving system is improved by four orders of magnitude to reach the level of 10^{-9} due to the small aperture stop, which

TABLE 1. Results of point spread function (PSF) ellipticity and PSF size

Rel Field of View	PSF Ellipticity: e	R (μm)	Coupling Efficiency (%)
0	0.0000	2.666	75.24
0.3	0.0699	2.819	67.73
0.5	0.1474	3.153	53.38
0.7	0.1226	3.275	60.01
1	0.1223	3.350	60.36

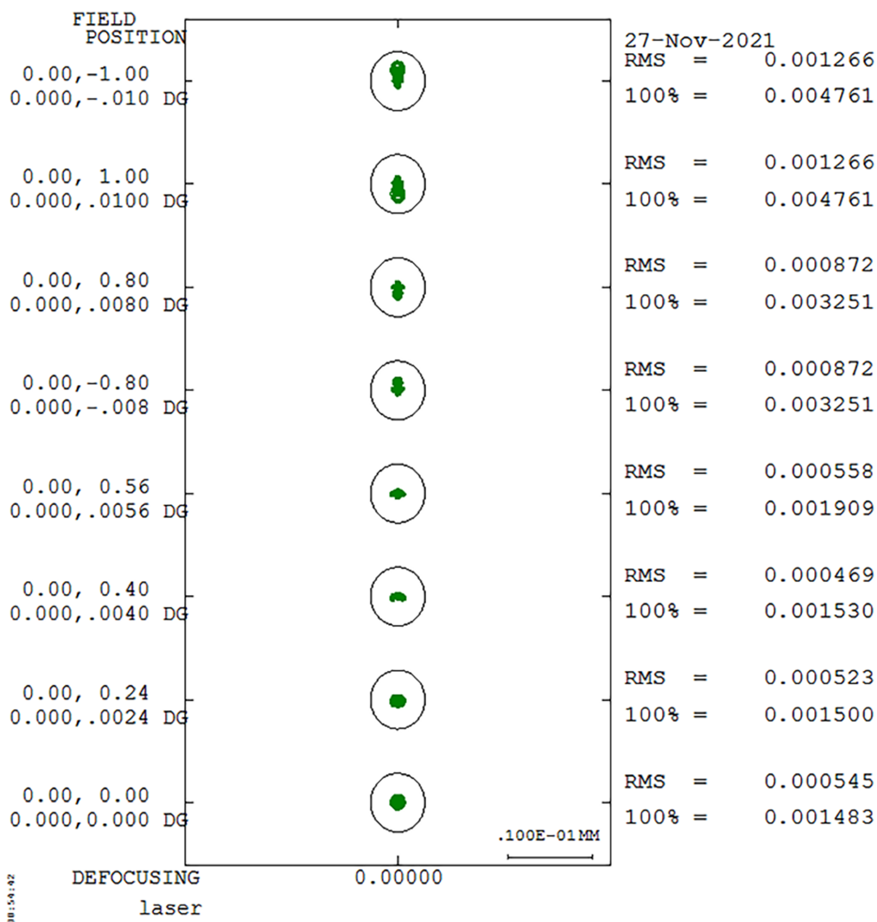

FIG. 8. Spots of the optical system.

effectively ensures the high sensitivity of the single-photon laser receiving system.

3.5. Tolerance Analysis

Tolerance analysis of the common aperture optical system was conducted, and the tolerance of each component is shown in Table 3. The probability density curves of the root mean square (RMS) wave front error (WFE) with the tolerance above are shown in Fig. 10. The system tolerance has engineering reliability.

3.6. Manufacture of Key Elements

The manufacture of primary mirrors and dichroic lenses are two challenges for common aperture systems. With the help of SPDT, the primary mirror (almost φ300 mm) made of aluminum alloy was well done. The RMS of the surface error reached 0.086 λ (λ = 632.8 nm), as shown in Fig. 11.

It was difficult to coat the dichroic lens in the development of the laser/infrared composite detection system. The average reflectance of the coated dichroic lens was better than 99.5% for 3.7–4.6 μm and 80% for 4.6–4.8 μm. At 1.064 μm, the transmittance was better than 96%. Considering the system assembly by the interferometer, which works at 0.6328 μm, the transmittance at 0.6328 μm was required to be better than 50%. The coating curves are shown in Figs. 12 and 13.

IV. MEASUREMENT EXPERIMENTS AND RESULTS

4.1. Close Target Imaging Test

To verify the imaging ability of the infrared system, a short-range imaging experiment was conducted by imaging buildings at a distance of 5 km. Figure 14 shows the test system. Figure 15 presents a test image in which the details of the target can clearly be distinguished and verifies the imaging resolution and nonuniformity of this system.

4.2. Distant Target Detection Test

Distant target detection is the main working mode of this system. In October 2020, a detection and tracking test of civil aviation aircraft was carried out in Qinghai, where the altitude is more than 3000 m and the air is thin. The temperature at the time of the test was 0 °C to −5 °C. The test equipment included a laser transmitting system and laser/MWIR receiving system. These two systems were integrated on the same two-dimensional turntable, so that the MWIR images could accurately guide the laser ranging

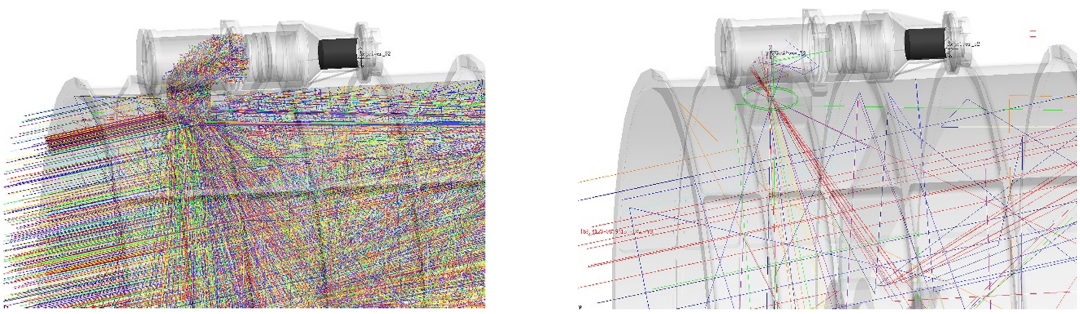

FIG. 9. Stray light simulation of the laser receiving system (left: without aperture stop; right: with aperture stop).

TABLE 2. Results of stray light simulation

θ (°)	10	20	30	40	50	60	70	80
PST-1 (E-05)	5.32	6.45	7.33	3.89	3.37	5.16	8.21	9.82
PST-2 (E-09)	1.64	2.52	4.64	1.75	0.56	0.14	0.15	0.16

TABLE 3. Table of tolerance allocation

Mirror	Radius of Curvature (mm)	Eccentricity Tolerance (mm)		Tilt Tolerance (")		Thickness/Spacing Tolerance (mm)
		X	Y	X	Y	
Primary Mirror	0.03	Assembly Datum				Spacing Between the Primary and Secondary mirrors: 0.05 Infrared lens: 0.02 Laser lens: 0.01
Secondary Mirror	0.02	0.01	0.01	30	30	
Infrared Lens Group	0.01	0.02	0.02	30	30	
Laser Lens Group	0.01	0.01	0.01	20	20	

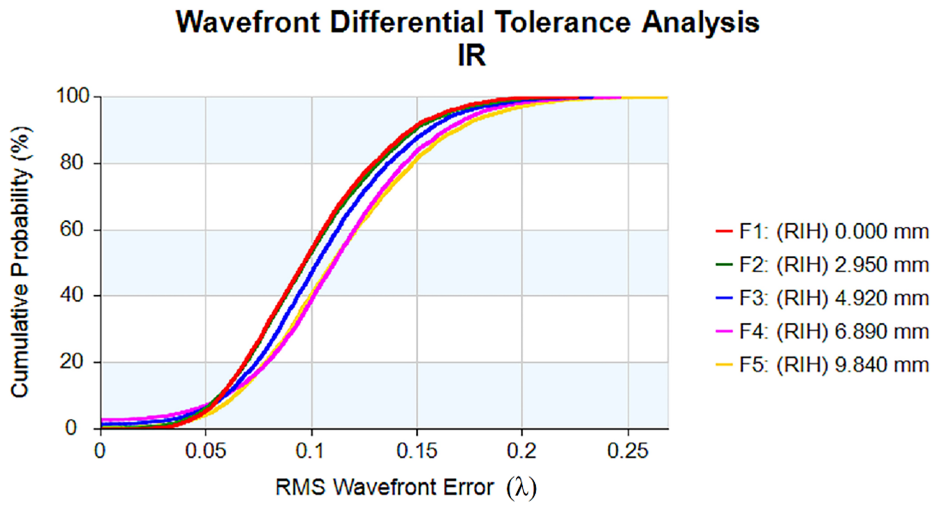

(a)

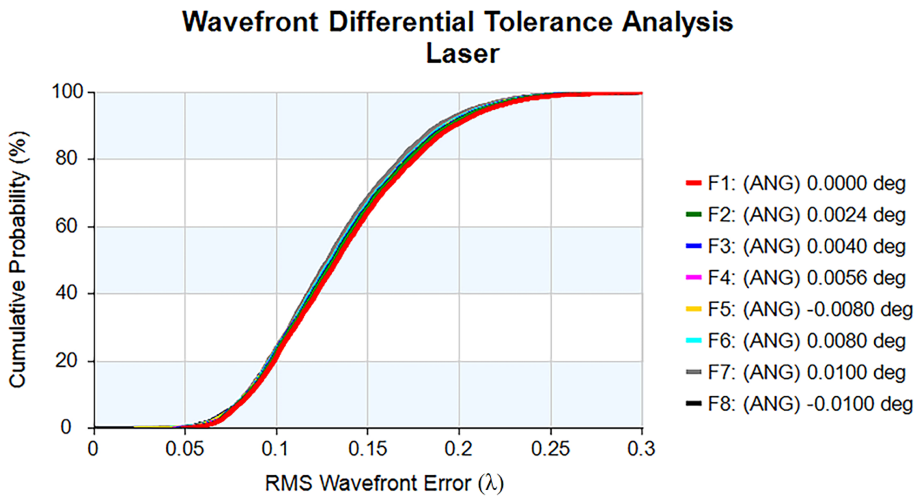

(b)

FIG. 10. Probability density curves of root mean square (RMS) wave front error (WFE) of (a) mid-wave infrared (MWIR) system and (b) laser receiving system by tolerance analysis.

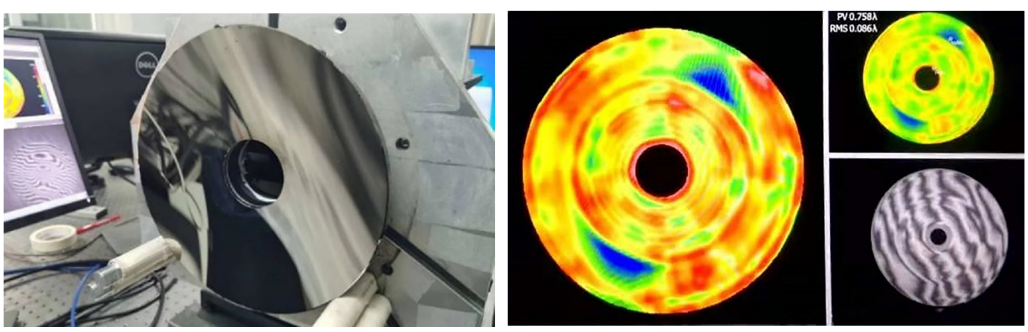

FIG. 11. Primary mirror and surface error results.

even when the target was in motion. The laser transmitting system was an independent unit and its axis was parallel to that of the laser/MWIR receiving system. The transmitting system used a 1064 nm pulse laser with a laser beam divergence angle of 0.5 mrad, pulse width of 8 ns and peak power of 40 MW. Figure 16 is a schematic diagram that illustrates how the tracking system works.

Figures 17–20 are laser ranging data and MWIR images

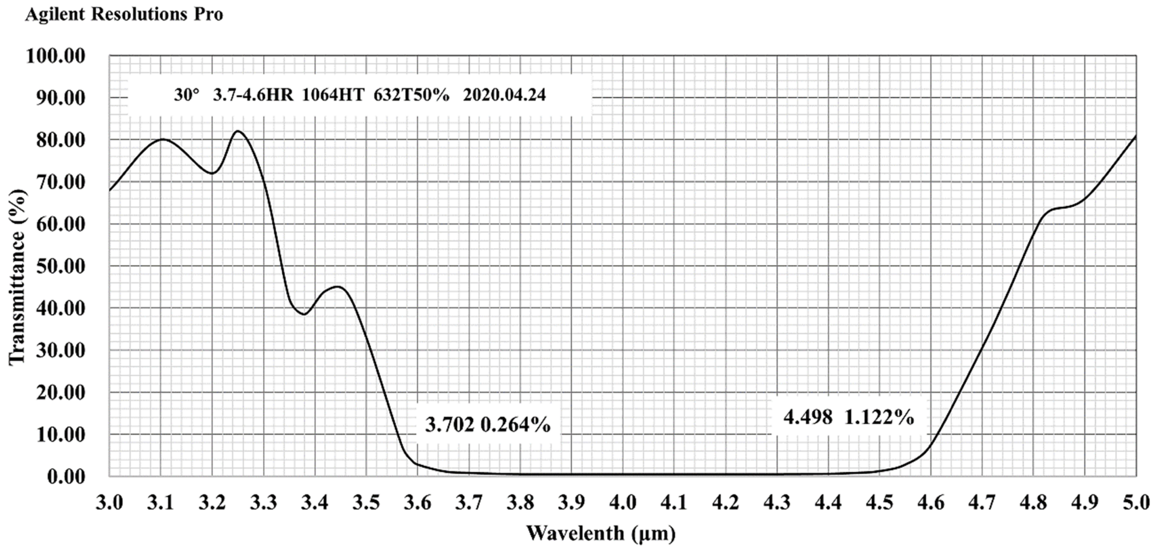

FIG. 12. Testing residual transmittance of the dichroic lens in mid-wave infrared (MWIR).

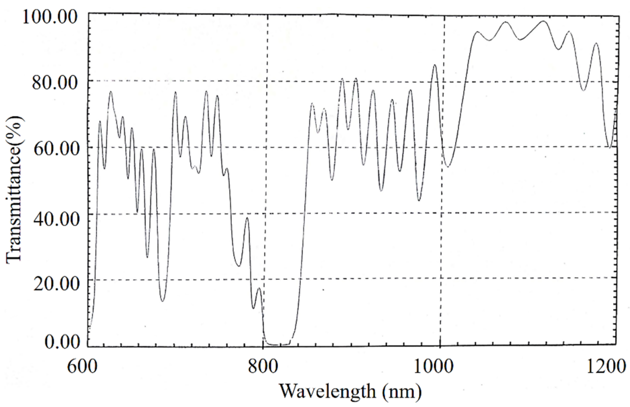

FIG. 13. Testing transmittance of the dichroic lens at visible and laser wavelengths (1.064 μm).

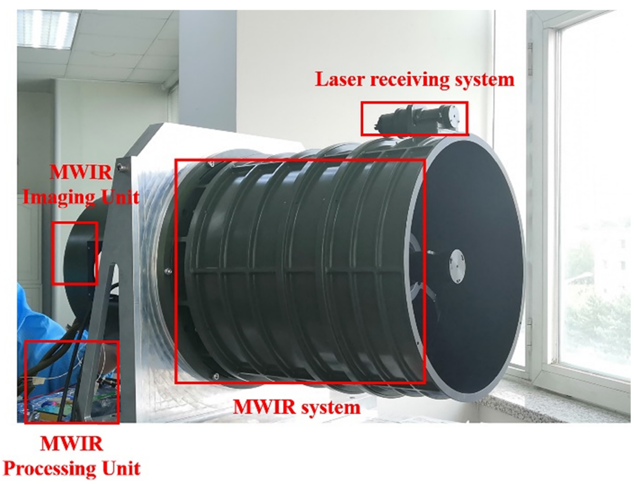

FIG. 14. The experiment system.

FIG. 15. Test image of building at 5 km distance (building of China Southern Airlines).

of the target with a pitch angle of 20°–35°. The test time was about 7 PM. The results showed that the visual axis of the laser/MWIR common aperture detection optical system had the advantages of high sensitivity and good stability. This system could be employed to effectively detect distant civil aviation aircraft, and the detection distance reached was over 225 km (SNR reached 15.8 at the expected value of 13 for the colder weather and higher radiation of the target) and 450 km (SNR reached 6.3 with the expected value of 5) with a ranging accuracy of 1 m.

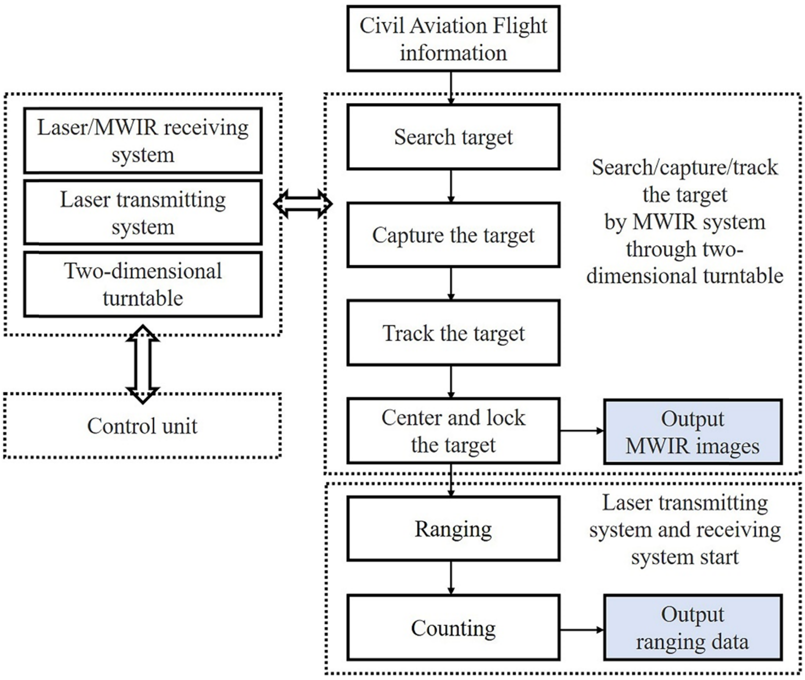

FIG. 16. Schematic diagram of the tracking system's working principle.

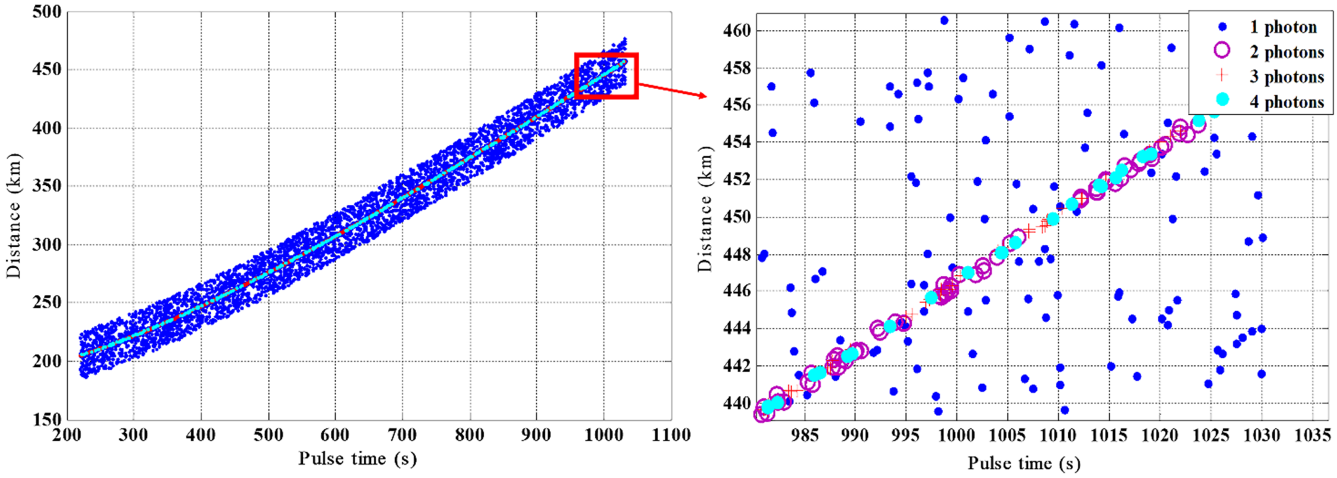

FIG. 17. The original ranging data.

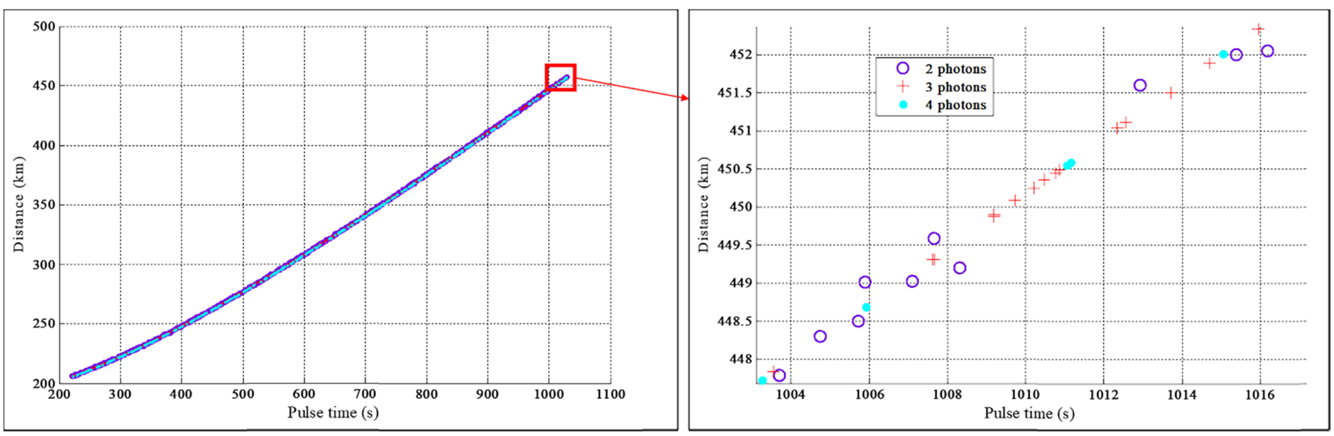

FIG. 18. The ranging data after filtering and mathematical statistics.

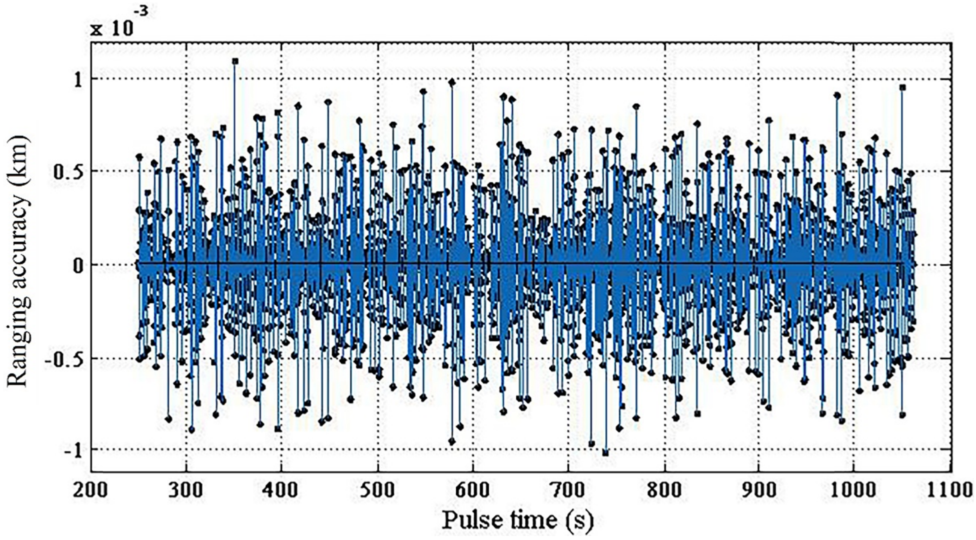

FIG. 19. Ranging accuracy after data fitting.

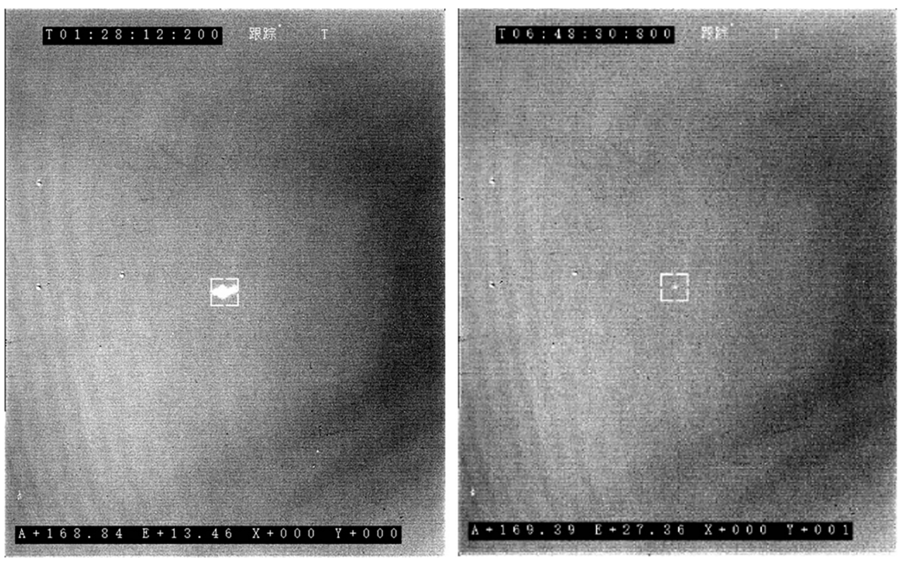

FIG. 20. Test image of civil aircraft at different distances of (a) 225 km and (b) 450 km.

V. CONCLUSION

In this paper, a single-photon laser ranging and medium-wave infrared common aperture detection system was proposed for the detection, tracking and ranging of distant civil aviation aircraft targets. This system was designed with the adoption of a secondary mirror as the dichroic component to achieve dual-band separation in the converging optical path. PSF ellipticity was introduced to evaluate the fiber coupling efficiency. Aperture diaphragm stray light elimination technology was proposed to improve the stray light suppression level of the single-photon laser receiving system by four orders of magnitude. The two key elements (the primary mirror and the dichroic lens) were well manufactured. As revealed from the experimental results, this system can achieve effective detection and tracking of distant civil aircraft with a distance of over 450 km (SNR = 6.3) and 1 m ranging accuracy, which can satisfy the demand for early warning detection and range measurement of distant targets in aviation, aerospace and ground detection.

FUNDING

National Natural Science Foundation of China (Grant No. 62005271).

ACKNOWLEDGMENT

We gratefully acknowledge the valuable cooperation of The 14th Research Institute of China Electronics Technol-

ogy Group Corporation in detection test.

DISCLOSURES

The authors declare no conflicts of interest.

DATA AVAILABILITY

Data underlying the results presented in this paper are not publicly available at the time of publication, which may be obtained from the authors upon reasonable request.

REFERENCES

1. L. Zhang, J. Lai, and Y. Huang, “Design of visible/long-wave infrared dual-band imaging optical system,” Proc. SPIE **10154**, 101540V (2016).
2. Z. Ma, H. Wang, Y. Shen, F. Wang, and Y. Xue, “Design of visible light / LWIR dual-band common aperture imaging optical system,” Proc. SPIE **11341**, 113410I (2019).
3. G. Chen, X. Qin, Y. Li, W. Xu, G. Shi, and X. Guo, “Optical design of an IR/SAL/MMW system with common aperture,” Electron. Opt. Control **27**, 98–102 (2020).
4. W.-W. Hu, Y.-L. Li, X.-K. Gu, Y.-P. Zhang, Y.-M. Zhang, and H.-X. Liu, “Remote laser ranging technology and its development,” Laser Infrared **49**, 273–281 (2019).
5. S. Song, “Research on key technologies of infrared and laser dual-mode compound detection,” Ph. D. Thesis, University of Chinese Academy of Sciences, Beijing, China (2017), pp. 15–16.
6. Z. Wang, “The research of the laser scanning and infrared compound detection,” M. S. Thesis, Xi’an Technological University, Xi’an, China (2013), pp. 57–66.
7. H. J. Cong, “Complex optical system design for infrared/laser with large field of view and high resolution,” M. S. Thesis, Harbin Institute of Technology, Harbin, China (2013), pp. 11–26.
8. R. Wang, “Compound guided system with active laser imaging and passive infrared imaging,” Chin. Opt. **6**, 536–543 (2013).
9. X. Liu, J. Chang, S. Feng, Y. Mu, X. Wang, and Z.-P. Xu, “Optical design of common-aperture multispectral and polarization optical imaging system with wide field of view,” Chin. Phys. B **28**, 084201 (2019).
10. Y.-J. Li, G. Jin, Y. Zhang, and L. Kong, “Co-aperture optical system for imaging and laser,” Chin. Opt. **8**, 220–226 (2015).
11. N. Yinand Y. Zhang, “Design of an active laser/infrared common aperture compound imaging optical system,” Infrared Technol. **38**, 77–80 (2016).
12. H.-W. Zhang, Y.-L. Ding, Y.-J. Ma, and W.-N. Chen, “Design of infrared dual-band/dual-FOV imaging early warning system,” Opt. Precis. Eng. **28**, 1283–1294 (2016).
13. Y. Luo, Y. He, L. Geng, M. Wang, L. Lei, Y. Wu, S. Hu, X. Hou, and W. Chen, “Long-distance laser ranging lidar based on photon counting technology,” Chin. J. Lasers **43**, 245–252 (2016).
14. S. G. Pan, “Research on remote laser ranging based on photon counting,” M.S. Thesis, Donghua University, Shanghai (2020), pp. 5–11.
15. S.-J. Chai, Z.-X. Tong, J.-X. Li, and C.-Z. Wang, “Infrared radiation characteristics and detection of stealth aeroplane,” Fire Control Command Control **39**, 26–29 (2014).
16. L. Kang, J. Zhao, Z. Li, Q. Zhou, and Q. Zhao, “The overview of the research work developments on infrared signature of aircrafts,” Infrared Technol. **39**, 105–115 (2017).
17. V. E. Zuev, “Signals and noise in laser ranging,” J. Sov. Laser Res. **8**, 283–426 (1987).
18. W.-J. Wang, J. Huang, G.-F. Yuan, and W.-T. Si, “Modeling and application analysis of operating range of air-based infrared system,” Opt. Precis. Eng. **28**, 1295–1302 (2020).
19. L. Y. Yu, H. G. Jia, Q. Wei, H. H. Jiang, T. Y. Zhang, and C. Wang, “A design of mid-wave infrared integral catadioptric optical system with wide FOV,” J. Opt. Soc. Korea **17**, 142–147 (2013).
20. X. Zhou, H. Sun, Q. Yuan, Z. Liu, H. Zhang, J. Wen, and Y. Wu, “Design of catadioptric infrared/laser compound seeker optical system,” J. Appl. Opt. **40**, 987–992 (2019).
21. J.-H. Lee, Y.-S. Jung, S.-Y. Ryoo, Y.-J. Kim, B.-U. Park, H.-J. Kim, S.-K. Youn, K.-W. Park, and H.-B. Lee, “Imaging performance analysis of an EO/IR dual band airborne camera,” J. Opt. Soc. Korea **15**, 174–181 (2011).
22. D. Jeong, J. H. Lee, H. Jeong, C. M. Ok, and H.-W. Park, “Infrared dual-field-of-view optical system design with electro-optic/laser common-aperture optics,” Curr. Opt. Photon **2**, 241–249 (2018).
23. J.-S. Xiang, G.-Q. Pan, and W.-H. Meng, Design of laser and infrared compound optical system,” Laser Infrared **48**, 104–108 (2018).